Supplement of Atmos. Meas. Tech., 16, 2753–2769, 2023
https://doi.org/10.5194/amt-16-2753-2023-supplement

Atmospheric Measurement Techniques
Open Access
EGU

Supplement of

The four-wavelength Photoacoustic Aerosol Absorption Spectrometer (PAAS-4λ)

Franz Martin Schnaiter et al.

Correspondence to: Franz Martin Schnaiter (martin.schnaiter@kit.edu)

Figure S1. Photograph of the PAAS-4λ consisting of the Optics Unit (lower left), the Flow Unit (upper left), and the Electronics Unit (right).

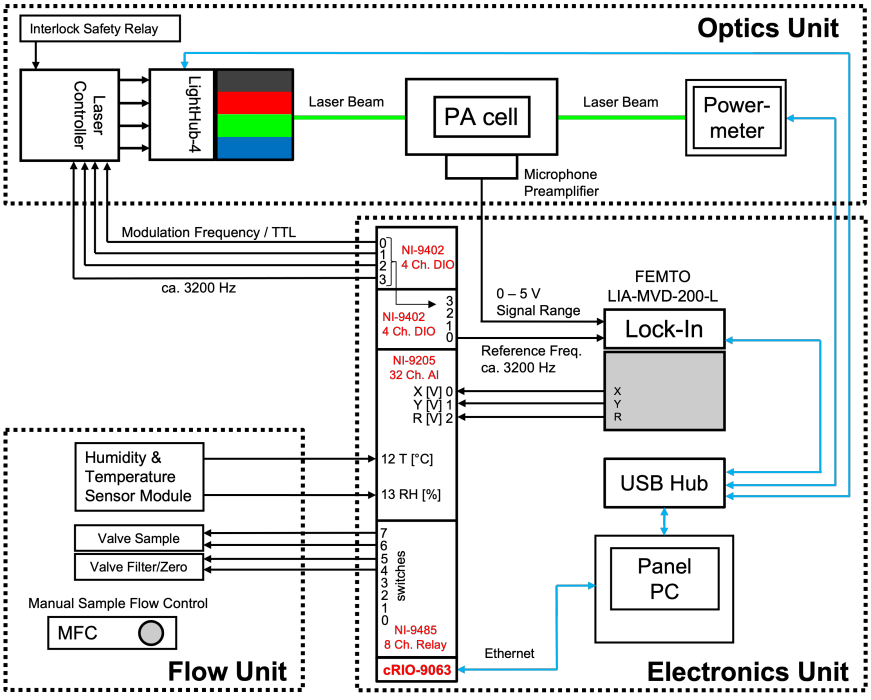

Figure S2. Schematics of the main components and their control and signal flows£ between the three units of PAAS-4λ.

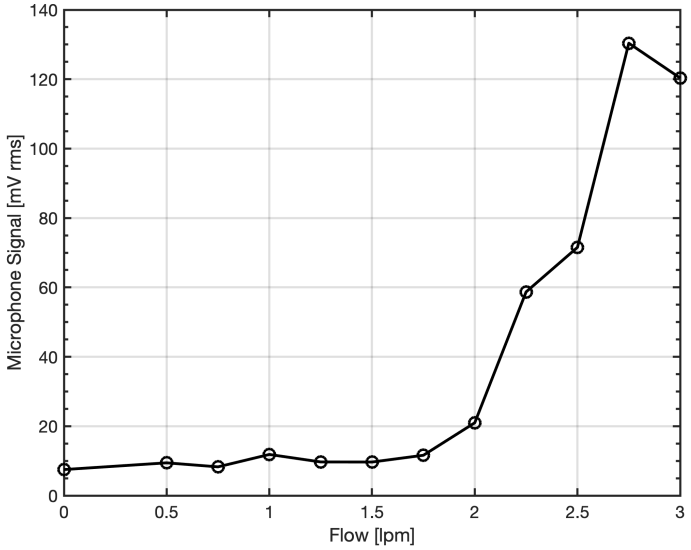

Figure S3. Microphone noise as a function of the air flow through the PA cell. The flow does not have an influence to the microphone noise up to a value of about 1.7 lpm.

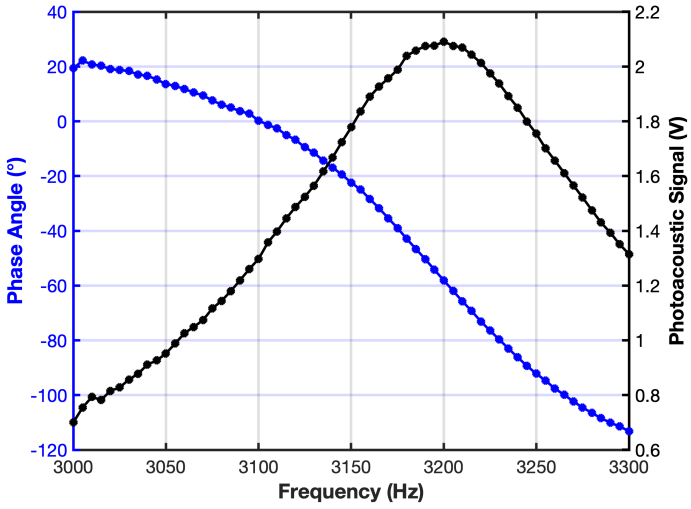

Figure S4. Frequency scan of the PA cell with 515 nm wavelength. The cell was filled with 907 ppb NO_2 during the scan. The PA resonator represents an underdamped harmonic oscillator with a damping frequency shift of about 40 Hz to lower frequencies.

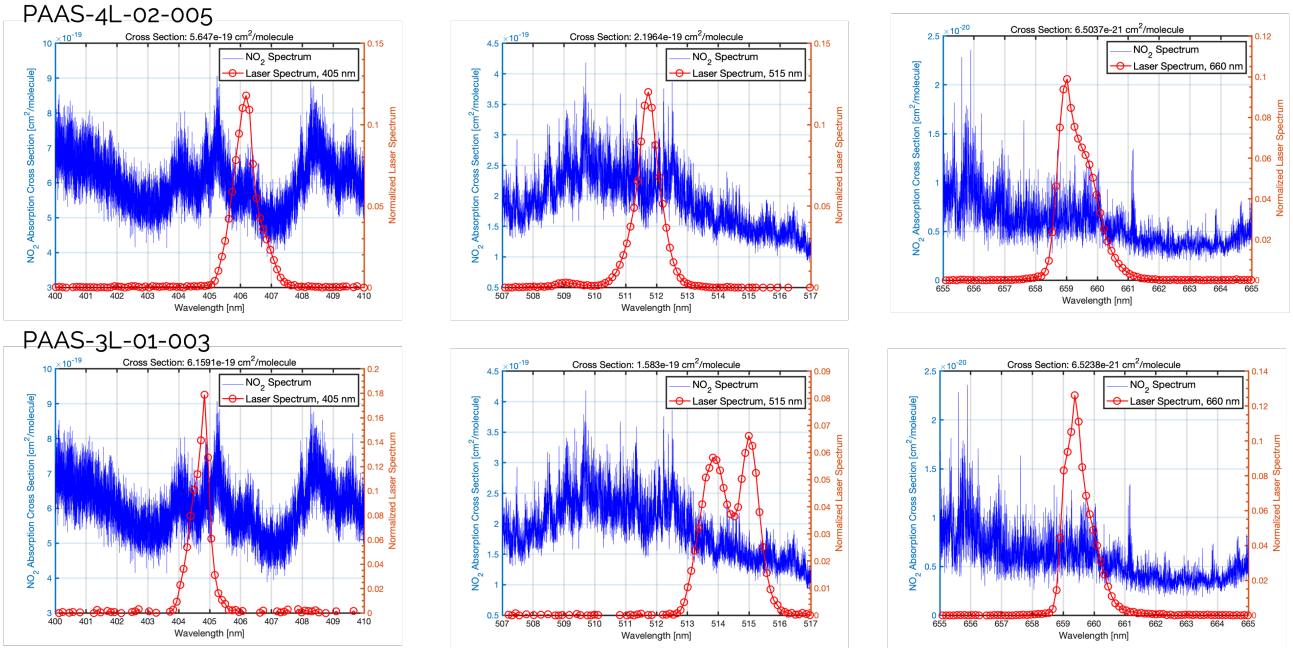

Figure S5. Comparison of measured laser emission spectra for laser units with manufacturer nominal wavelengths of 405 nm (left), 515 nm (middle), and 660 nm (right). The lasers are implemented in two PAAS-4λ units with serial numbers PAAS-4L-02-005 (hosting 405, 473, 515, and 660 nm lasers, top) and PAAS-3L-01-003 (hosting 405, 515, and 660 nm lasers, bottom). The emission spectra are convolved with the high resolution NO_2 spectrum from Vandaele et al. (2002) to determine the laser-specific NO_2 absorption cross section. Differences up to 40% in the laser-specific NO_2 absorption cross section can occur that directly translate into the calibration accuracy in case the laser-specific cross section is not deduced for each laser unit.

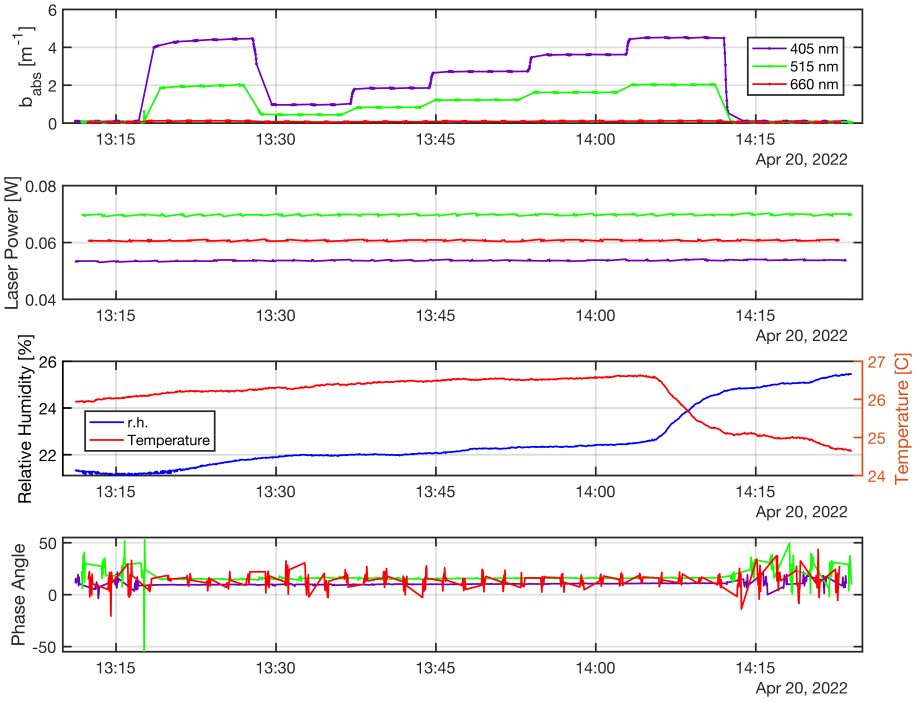

Figure S6. Temporal evolution of the PAAS-4λ measurement data during a calibration procedure with NO_2. The individual panels show from top to bottom the raw lock-in amplifier output, the power of the (modulated) laser emissions, the relative humidity and temperature in the laboratory, and the phase angle of the raw lock-in signal. Note that the PAAS unit used in this measurement (S/N PAAS-3L-01-003) consists of only three wavelengths. See text for details.

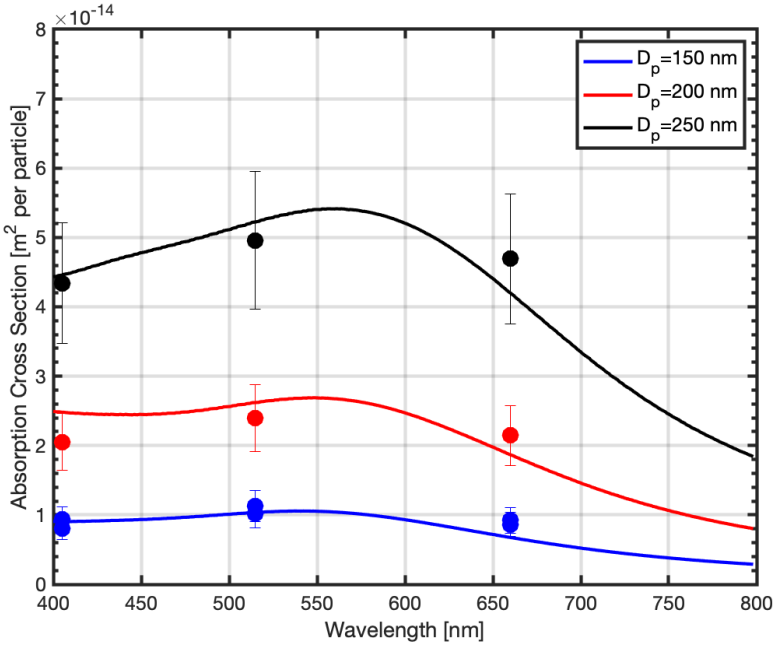

Figure S7. Absorption cross section spectrum of Nigrosin particles for three different diameters, 150 nm (blue), 200 nm (red), and 250 nm (black). Measured cross sections deduced from PAAS-4λ and CPC data are given by the filled circular symbols. Simulated spectra using Mie Theory are represented by the lines. Note that the PAAS unit used in this measurement (S/N PAAS-3L-01-003) consists of only three wavelengths.

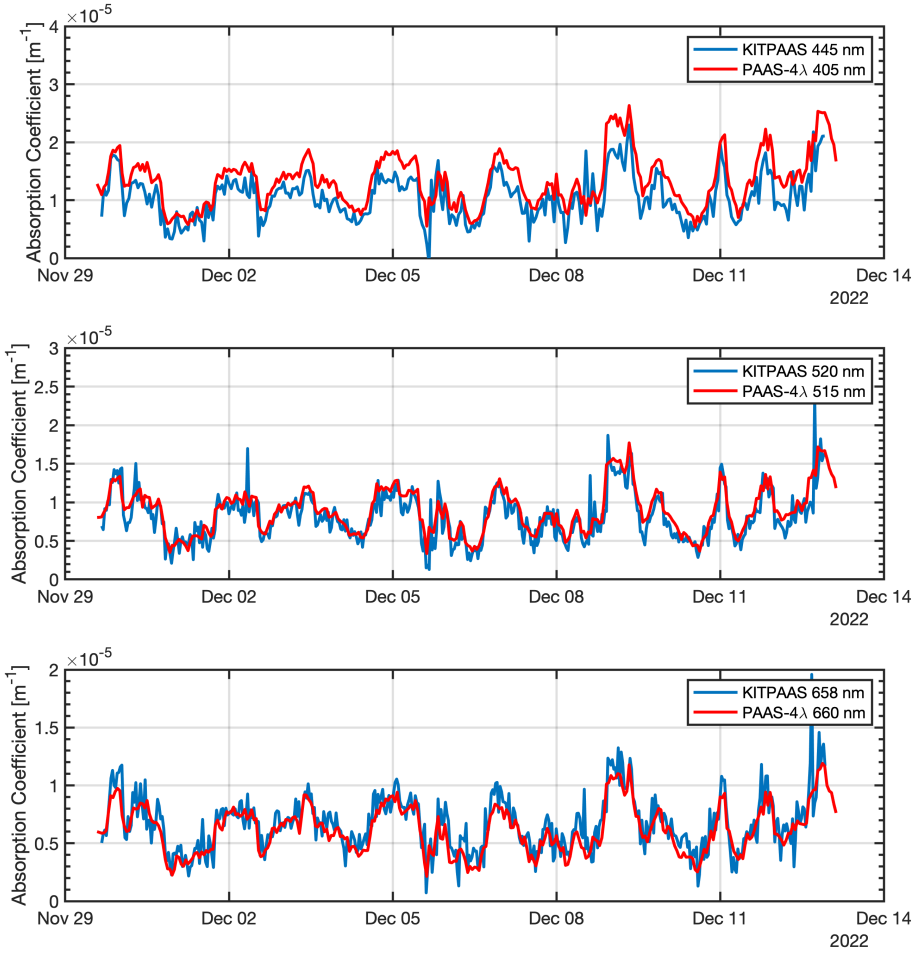

Figure S8. Comparison of the absorption coefficients measured by a PAAS-4λ unit (PAAS-3L-01-002 with 405, 515, 660, and 785 nm lasers) with the three-wavelength prototype instrument version KITPAAS described in Linke et al. (2016). The comparison demonstrates the significantly improved noise of PAAS-4λ. Each data set is averaged over 1h.

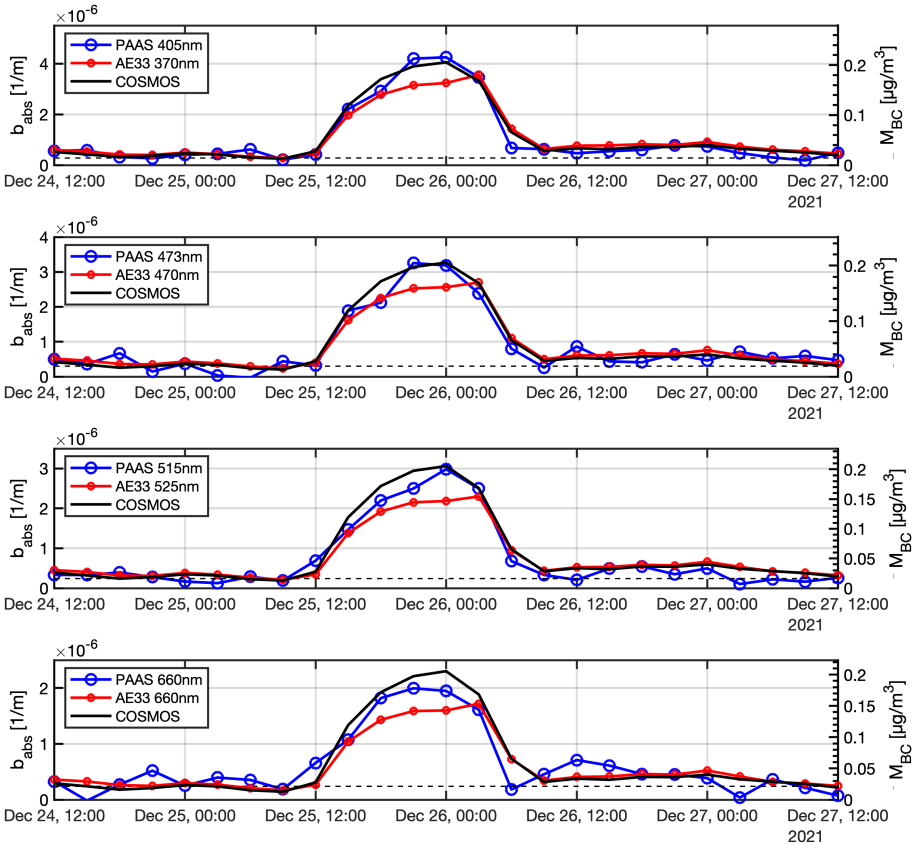

Figure S9. Comparison of the absorption coefficients b_{abs} measured by PAAS-4λ and the Aethalometer (AE33) with the BC mass concentration M_{BC} from the COSMOS for an approximately one day pollution period on December 26, 2021. AE33 coefficients are corrected with the C values deduced for the complete deployment period in Fig. 12. The COSMOS BC mass concentration axis is scaled to the b_{abs} axis according to the MAC values deduced from the PAAS-4λ/COSMOS correlation analysis for the complete period in Fig. 10.